Spectral Analysis for Nonstationary and Nonlinear Systems: A Discrete-Time-Model-Based Approach

Fei He, Stephen A. Billings*, Hua-Liang Wei, Ptolemaios G. Sarrigiannis, and Yifan Zhao

***Abstract*—A new frequency-domain analysis framework for nonlinear time-varying systems is introduced based on parametric time-varying nonlinear autoregressive with exogenous input models. It is shown how the time-varying effects can be mapped to the generalized frequency response functions (FRFs) to track nonlinear features in frequency, such as intermodulation and energy transfer effects. A new mapping to the nonlinear output FRF is also introduced. A simulated example and the application to intracranial electroencephalogram data are used to illustrate the theoretical results.**

***Index Terms*—Frequency response functions (FRFs), nonlinear and nonstationary systems, spectral analysis, system identification, time-varying systems.**

I. Introduction

In the field of signal processing and systems engineering, it is well known that the output spectrum of a linear time-invariant (LTI) system is equal to the product of the input spectrum with the system frequency response function (FRF). This analytical relationship has been widely applied for systems analysis, controller and filter design, fault detection, and vibration analysis. However, many real systems are nonlinear. The frequency-domain analysis of a nonlinear time-invariant (NTI) system is mainly based on the concept of generalized FRFs (GFRFs) [1] that extend the linear FRF concept to a wide class of nonlinear systems. The estimation of GFRFs was originally obtained from multidimensional Fourier transformation of Volterra series models [2], [3], and later parametric approaches based on nonlinear differential equation and nonlinear autoregressive moving average with exogenous input (NARMAX) models [4]–[6] have been proposed, which are computationally more attractive. Recently, the classical linear frequency-domain relationship has been extended by deriving an analytical expression relating the input and output spectra of NTI systems based on the output FRF (OFRF) [7], [8]. The OFRF is an important development that facilitates the spectral analysis of a class of NTI systems.

Nevertheless, many real systems exhibit nonstationarity or time-varying behavior, including a large number of physical, physiological, and biochemical signals and systems [9]. Identification of linear time-varying (LTV) systems has been extensively studied in the time domain [10], [11], and the identified LTV model can be mapped in to the frequency domain [12], which is important for system analysis especially for real applications. For example, time-varying autoregressive (AR), autoregressive moving average (ARMA), or autoregressive with exogenous input (ARX) models have been applied for time–frequency analysis of electrophysiological signals (electroencephalogram (EEG), electromyogram (EMG), etc.) [13]–[16]. Although such LTV models can be applied to approximate nonlinear systems with relatively slow and smooth nonstationarities to provide good estimation and tracking results in real-time applications [17], [18], in the frequency domain, these methods fail to reproduce nonlinear effects such as harmonics, intermodulations and energy transfer that can only be produced from nonlinear models. However, there are very few studies (see, e.g., [19] and [20]) for the modeling and identification of nonlinear and nonstationary systems, and the important frequency-domain analysis of such systems does not appear to have been investigated in the literature. These are important and challenging problems that will be investigated in this study.

In this paper, nonlinear and nonstationary dynamic systems are modeled using polynomial time-varying nonlinear autoregressive with exogenous input (NARX) (TV-NARX) models and the identified models are then transformed and analyzed in the frequency domain based on the new concept of time-varying GFRFs (TV-GFRFs). More importantly, it is shown that the high-dimensional TV-GFRFs can be transformed and visualized in a two-dimensional time–frequency space, based on a novel analysis of "features" in the TV-GFRFs. The fundamental relationship between the input and output time-dependent spectra is also derived to generalize the time-invariant OFRF theory to the nonstationary case. The theories are illustrated using a simulated nonstationary and nonlinear system, and a real intracranial EEG recording.

II. Modeling of Time-Varying Nonlinear Systems

A wide variety of nonlinear systems can be represented using the NARMAX model [21]. The deterministic part of the NARMAX model is an "NARX" model that can be expressed

Manuscript received October 31, 2012; revised January 17, 2013 and March 5, 2013; accepted March 5, 2013. Date of publication March 12, 2013; date of current version July 13, 2013. This work was supported by the Engineering and Physical Sciences Research Council (EPSRC), U.K., and by the European Research Council (ERC) Advanced Investigator Grant.

F. He, H.-L. Wei, and Y. Zhao are with the Department of Automatic Control and Systems Engineering, The University of Sheffield, Sheffield, S1 3JD, U.K. (e-mail: f.he@sheffield.ac.uk; w.hualiang@sheffield.ac.uk; y.zhao@sheffield.ac.uk).

*S. A. Billings is with the Department of Automatic Control and Systems Engineering, The University of Sheffield, Sheffield, S1 3JD, U.K. (e-mail: s.billings@sheffield.ac.uk).

P. G. Sarrigiannis is with the Department of Clinical Neuophysiology, Sheffield Teaching Hospitals NHS Foundation Trust, Royal Hallamshire Hospital, Sheffield, S10 2JF, U.K. (e-mail: Ptolemaios.Sarrigiannis@sth.nhs.uk).

as the following nonlinear difference equation:

$$y(t)=f\left(y(t-1),\ldots,y(t-n_y),u(t-1),\ldots u(t-n_u)\right)+e(t) \tag{1}$$

where f is a nonlinear function, $u(t)$ and $y(t)$ the input and output sequences, with maximum lags n_u and n_y, respectively; $e(t)$ is the model prediction error or a noise sequence that is assumed zero mean and independent. Here, t represents discrete time. For many practical problems, the nonlinear function $f(\cdot)$ is generally unknown. Polynomial functions are most commonly used to approximate the unknown $f(\cdot)$, as the resulting polynomial NARX model [22] can be expressed as a linear-in-the-parameter form, so that $y(t)=\varphi^T(t)\theta+e(t)$. Here, $\varphi(t)$ is the regressor vector containing monomials of lagged input and output terms, and θ is the parameter vector. For colored noise situations, stochastic "moving-average" model terms need to be included into (1), which yields the NARMAX model. Estimation based on the NARMAX model [23] involves iteratively computing and modeling the prediction errors at each step. When modeling a time-varying system, a TV-NARX model is required by replacing the time-invariant parameter vector θ with a time-varying parameter vector $\theta(t)$. The polynomial TV-NARX can be expressed as

$$\begin{aligned} y(t) &= \sum_{n=1}^{M} y_n(t)+e(t) \\ y_n(t) &= \sum_{p=0}^{n}\sum_{k_1,k_{p+q}=1}^{K} c_{p,q}(k_1,\ldots,k_{p+q},t) \\ &\quad\times\prod_{i=1}^{p} y(t-k_i)\prod_{i=p+1}^{p+q} u(t-k_i) \\ &= \varphi^T(t)\theta(t) \end{aligned} \tag{2}$$

where $y_n(t)$ is the nth-order output of the system and M is the order of the nonlinearity, with $p+q=n, k_i=1,\ldots,K, \sum_{k_1,k_{p+q}=1}^{K}\equiv\sum_{k_1=1}^{K}\cdots\sum_{k_{p+q}=1}^{K}$. The time-varying parameter vector is $\theta(t)=[c_{0,1}(1,t),\ldots,c_{0,1}(K,t),c_{1,0}(1,t),\ldots,c_{p,q}(K,\ldots,K,t)]^T$. The linear TV-AR or TV-ARX models are special cases of the TV-NARX model where only linear output or linear input–output terms are present in (2). Equation (2) is a linear-in-the-parameter model, but can consist of a large number of candidate terms. The number of model terms increases as the order of input and output terms (q and p) and the corresponding maximum lags (K) increase.

Two approaches have been investigated for model selection and identification of the TV-NARX model. The first approach uses recursive estimation and is based on applying model selection techniques over windows of the data to determine the overall nonstationary model structure. The other approach expands the time-varying model parameters using basis functions so that the identification is mapped to a time-invariant problem. More specifically, the first approach divides the input–output time series into several subintervals. For each segment, a time-invariant model (e.g., NARX) is applied and the model structures can be determined by using, for example, forward regression with orthogonal least squares (FROLSs) [23], [24]. Then, by combining the selected model terms from different intervals, a "common" model structure can be determined. Recursive algorithms, for example, recursive least squares (RLSs) or least mean squares (LMSs), can then be used to estimate the time-varying parameters. An alternative approach is based on expanding the time-varying parameters $\theta(t)$ using basis function approximations, such as multiwavelet basis functions, which have recently been employed in linear TV-AR, and TV-ARX model identification [25]–[28]. The model selection algorithm (e.g., FROLS) can then be applied to the expanded time-invariant model, and the relevant time-varying parameters in the original model can therefore be selected and estimated. Because (2) is in a linear-in-the-parameter structure, the model selection and estimation algorithm proposed for linear cases (see [13] and [28]) can be adapted to TV-NARX models. Therefore, a detailed identification algorithm is not provided here.

In most cases, both the approaches can identify the TV-NARX models and track the time-varying parameters, but the latter approach can estimate and track very rapid changes in the time-varying parameters more accurately and with smaller estimation variances [26], [28]. The latter approach is also theoretically more elegant because the FROLS together with Bayesian information or related criteria (see [13]) can be used to determine the complexity and structure of the expanded model as well as the original time-varying model. As a result, the nonlinearity and nonstationarity detection problem can be solved simultaneously and automatically as part of the identification process, since the LTV (e.g., TV-ARX) and NTI (e.g., NARX) models are just special cases of the TV-NARX model. However, for large-scale problems (for example, models with very high-order dynamics or a very large number of regression terms), the second approach can be computationally more costly as the number of expanded model terms would be large for model selection.

III. Time-Varying Nonlinear FRFs

Compared to time-domain identification, the frequency-domain analysis of nonlinear time-varying systems is a challenge that does not appear to have been studied in the literature. However, tracking nonlinear frequency-domain features is a fundamentally important and unsolved problem in many applications. Although several time–frequency measures, such as mutual information, synchronization measures, and wavelets, have been applied for nonlinear data like EEG signal analysis [29], [30], these nonparametric approaches cannot provide any links back to the time-domain behaviors and modeling. Links from time to frequency and vice versa can be very important in the analysis of complex phenomena such as EEG data analysis. Such links can be established by using the method to be introduced in this section. As an extension of linear FRF, the frequency-domain analysis of NTI systems is mainly based on GFRF theory. The nth-order GFRF is defined as the multiple Fourier transform of the nth-order Volterra kernel

$$\begin{aligned} &H_n(f_1,f_2,\ldots,f_n) \\ &=\int_0^{\infty}\cdots\int_0^{\infty} h_n(\tau_1,\tau_2,\ldots,\tau_n)e^{-j2\pi(f_1\tau_1+\cdots+f_n\tau_n)}d\tau_1\ldots\tau_n \end{aligned} \tag{3}$$

where $h_n(\tau_1, \tau_2, \ldots, \tau_n)$ is the nth-order Volterra kernel and $f_1, f_2, \ldots, f_n$ represents an n-dimensional frequency hyperspace. The concept of GFRFs, based on Volterra series theory [31], can be extended to the NARX model [4]–[6]. The general expression of the GFRFs for a time-invariant NARX model is given in [32]. The GFRFs are functions of the NARX model parameters, while the structure of the GFRF expression purely depends on the NARX model structure. Therefore, when only parametric time-varying effects (without considering time variation in the model structure) are taken into account that is the case in this study, previous results obtained based on NARX models can be extended to TV-NARX cases. An extra time dimension t needs to be introduced to accommodate the parametric time-varying effects and then the time-varying parameters can be regarded as "constants" in a local region without affecting the model structure, and thus, the formulations of GFRFs. As a result, the nth-order TV-GFRF with respect to a TV-NARX model (2) can be expressed as

$$H_n(f_1, \ldots, f_n, t) = \frac{H_{n[u]}(f_1, \ldots, f_n, t) + H_{n[y]}(f_1, \ldots, f_n, t) + H_{n[uy]}(f_1, \ldots, f_n, t)}{1 - \sum_{k_1=1}^{K} c_{1,0}(k_1, t) e^{(-j2\pi(f_1 + \cdots + f_n)k_1/f_s)}} \tag{4}$$

where f_s is the sampling frequency and the contributions of the pure input, output, and cross-product nonlinearities $H_{n[u]}, H_{n[y]},$ and $H_{n[uy]}$, respectively, are defined as

$$H_{n[u]}(f_1, \ldots, f_n, t) = \sum_{k_1, k_n=1}^{K} c_{0,n}(k_1, \ldots, k_n, t) e^{-j2\pi(f_1 k_1 + \cdots + f_n k_n)/f_s}$$

$$H_{n[y]}(f_1, \ldots, f_n, t) = \sum_{p=2}^{n} \sum_{k_1, k_n=1}^{K} c_{0,n}(k_1, \ldots, k_n, t) H_{n,p}(f_1, \ldots, f_n, t)$$

$$H_{n[uy]}(f_1, \ldots, f_n, t) = \sum_{q=1}^{n-1} \sum_{p=1}^{n-q} \sum_{k_1, k_{p+q}=1}^{K} c_{p,q}(k_1, \ldots, k_{p+q}, t) \times H_{n-q,p}(f_1, \ldots, f_{n-q}, t) \times \exp[-j2\pi(f_{n-q+1}k_{n-q+1} + \cdots + f_{p+q}k_{p+q})/f_s] \tag{5}$$

The contribution of the pth-order nonlinearity in $y(t)$ to the nth-order GFRF $H_{n,p}(\cdot)$ can be recursively computed according to [32] as

$$H_{n,p}(\cdot) = \sum_{i=1}^{n-p+1} H_i(f_1, \ldots f_i, t) H_{n-i,p-1}(f_{i+1}, \ldots, f_n, t) \times \exp[-j2\pi(f_1 + \cdots + f_i)\, k_p/f_s]. \tag{6}$$

The aforementioned recursion finishes with $p = 1$, where the $H_{n,1}(f_1, \ldots, f_n, t)$ is defined as

$$H_{n,1}(f_1, \ldots, f_n, t) = H_n(f_1, \ldots, f_n, t) \times \exp[-j2\pi(f_1 + \cdots + f_i)\, k_1/f_s]. \tag{7}$$

When analyzing the linear frequency response or the first-order GFRF of a nonlinear system, the main interest is to identify the "peaks" in the frequency response, because these indicate at which frequency ranges the output response will be stronger. When analyzing a higher order GFRF of a nonlinear system, it is not only the "peaks" but more importantly the "ridges" where the gains of the GFRF reach their maxima. The locations of the "ridges" indicate the transfer of energy from input spectral components to the output spectra at their summation, to produce strong intermodulation, harmonic, or significant dc shift effects in the output [33]–[35].

By analyzing the general expressions of the nth-order TV-GFRFs in (4), and according to the characteristic analysis of GFRFs given by [36], [37], it will be demonstrated that the directions of the "ridges" mainly depend on the NARX model structure, and are rarely affected by time-varying effects of one or a few parameters. Nevertheless, the positions and the magnitudes of the "ridges" do rely on the model parameters. This result is summarized in Proposition 1.

Proposition 1: The directions and positions of the "ridges" in the nth-order GFRF gain profile only depend on the factors in the denominator of the nth-order GFRF. There always exist "ridges" along the $f_1 + f_2 + \cdots + f_n = C_i$ direction, and often with extra "ridges" along the "off-diagonal" directions of those subspaces in the n-dimensional frequency domain, i.e., $f_j = C_i, f_j + f_{j+1} = C_i, \ldots, f_1 + \cdots + f_{j+n-2} = C_i$, with $j \in \{1, \ldots, n\}$ depending on the model structure. The directions of the "ridges" mainly depend on the NARX model structure, while the positions of the "ridges" only depend on the parameters of the linear output terms. The magnitudes of the "ridges" can depend on all the parameters of the NARX model.

Proof: According to [36], the factors in the denominator jointly determine the maxima of the nth-order GFRF. Since the "ridges" are a subset of the maxima, only the denominator is required to be analyzed. By substituting (5)–(7) into (4), the denominator of the nth-order GFRF can be expressed as

$$\prod_{i=1}^{n} \left(1 - \sum_{k_1=1}^{K} c_{1,0}(k_1, t) \exp[-j2\pi k_1 f_i/f_s]\right) \times \prod_{i=1}^{n-1} \left(1 - \sum_{k_1=1}^{K} c_{1,0}(k_1, t) \exp[-j2\pi k_1 (f_i + f_{i+1})/f_s]\right) \times \cdots \times \left(1 - \sum_{k_1=1}^{K} c_{1,0}(k_1, t) \exp[-j2\pi k_1 (f_1 + \cdots + f_n)/f_s]\right). \tag{8}$$

Since the denominator (8) is a product of all the parts, at a specific time and frequencies when the gain of any of the parts reaches a minimum, the overall gain of the GFRF will reach a large value. A subset of these "large values" will appear as a "ridge" in the GFRF gain plot. As long as the nth-order GFRF exists, the last part in (8) always exists (as defined in (4)), while other parts may appear depending on the NARX model structure. For some cases, only the last part in the denominator (8) exists, if: 1) there are no linear input terms (i.e., $u(t - k_1)$), or 2) there are linear input terms, but there exist only pure nonlinear

input terms without any other nth-order nonlinear terms. For the above two cases, the "ridges" in the nth-order GFRF are always along the direction defined by $f_1 + f_2 + \cdots + f_n = C_i$, where the constants C_i determine the position of the ridges when the last part of (8) reaches a minimum, that is,

$$C_i = \arg \min_{f_1+f_2+\cdots+f_n} \left| 1 - \sum_{k_1=1}^{K} c_{1,0}(k_1, t) \exp[-j2\pi k_1 (f_1+f_2+\cdots+f_n)/f_s] \right| \quad (9)$$

It is obvious that the positions of the ridges only depend on the parameters of the linear output terms, since C_i only functionally depends on $c_{1,0}(k_1, t)$ in (9) when the model structure (i.e., k_1) is fixed, which is also true for other ridges in other parts of (8). It is also straightforward to demonstrate that if there is only one linear output delay term (i.e., $K = 1$) in the model, $C_i = 0$. Otherwise, if there are more than one linear output terms, C_i can be nonzero. Moreover, if there are linear input terms in the model, and either cross-product or pure output nonlinear terms exist, then the other parts in (8) would be present together with the last part as a direct result of GFRF expression (4). Hence, extra ridges in the subspaces, e.g., $f_1 = C_i$ and/or $f_2 = C_i$, can be observed additional to the ridges along $f_1 + f_2 + \cdots + f_n = C_i$, and this proves the dependency of ridge directions on the model structure. In addition, the magnitudes of the ridges are affected by both the gains of the denominator and the numerator in (4), and the magnitudes depend on all the model parameters up to nth order. ■

Proposition 1 indicates the most common and important ridge of an nth-order (TV)-GFRF is along the $f_1 + f_2 + \cdots + f_n = C_i$ direction, and the position of this ridge denotes at which frequency combinations the intermodulation effects are significant. Since the ridge direction only depends on the (TV-)NARX model structure, in order to analyze and visualize the parametric time-varying effects on the nth-order TV-GFRF, the gain or phase of the nth-order TV-GFRF can be averaged along the ridge direction $f_1 + f_2 + \cdots + f_n = C_i$ as

$$\begin{cases} \left|H_n^{f_1+f_2+\cdots+f_n}(f,t)\right| \\ \quad = \displaystyle\int_{f_1+f_2+\cdots+f_n=f} \frac{1}{N_f} \left|H_n(f_1,\ldots,f_n,t)\right| df \\ \measuredangle H_n^{f_1+f_2+\cdots+f_n}(f,t) \\ \quad = \displaystyle\int_{f_1+f_2+\cdots+f_n=f} \frac{1}{N_f} \measuredangle H_n(f_1,\ldots,f_n,t) df \end{cases} \quad (10)$$

where $\measuredangle$ denotes phase. As a result, the high-dimensional TV-GFRFs can be visualized and analyzed in a two-dimensional time–frequency space. Any elements in (10) with relatively high magnitudes (or large gain values) would indicate potential significant intermodulation effects in the output at those specific frequencies and times with the contribution from the nth-order nonlinearity. These results greatly facilitate the understanding and analysis of the frequency characteristics of a nonlinear and nonstationary system.

IV. Spectral Analysis: Time-Varying OFRFs

Spectral analysis for linear systems is a well-established and widely used tool in signal processing. It is well known that the output frequency response of a stable LTI system can be expressed as $Y(f) = H(f)U(f)$, where $U(f)$ and $Y(f)$ are the Fourier transforms of the system input and output time series $u(t)$ and $y(t)$, respectively. For a time-varying linear system, this simple relationship still holds [12] although the extra time dimension (t) is introduced

$$Y(f,t) = H(f,t)U(f,t). \quad (11)$$

Hence, the input and output spectra as well as the time-dependent FRF are in three-dimensional (3-D) time–frequency spaces. Because of the linear nature of an LTV system, the output spectrum $Y(f,t)$ only contains the same frequencies as the input spectrum $U(f,t)$, although the magnitudes with respect to each frequency can be time dependent due to the time-varying effects.

For an NTI system, the relationship between system input and output spectra is more complicated. An analytical expression has been proposed as an extension to the well-known linear relationship and is referred to as the OFRF [8]. In this paper, the OFRF concept is further extended to the more general nonlinear time-varying (nonstationary) case. The expression for the time-varying OFRF (TV-OFRF) of a nonlinear time-varying system is given by

$$\begin{aligned} Y(f,t) &= \sum_{n=1}^{N} Y_n(f,t) \\ Y_n(f,t) &= \frac{1}{\sqrt{n}} \int_{f_1+\cdots+f_n=f} H_n(f_1,\ldots,f_n,t) \\ &\quad \times \prod_{i=1}^{n} U(f_i,t) df. \end{aligned} \quad (12)$$

Equation (12) is a natural generalization of the LTV relationship (11) and time-invariant OFRF concept. The nth-order TV-GFRF $H_n(f_1,\ldots,f_n,t)$ can be obtained from the identified TV-NARX model using (4), and integrated over the n-dimensional hyperplane $f_1 + \cdots + f_n = f$ with the input spectrum to provide the nth-order TV-OFRFs. For nonlinear time-varying systems, the relationship between input and output spectra is more complicated than the linear case and new frequencies can often be produced in the output. Intermodulation, harmonic, or energy transfer effects are often observed in the output spectrum, due to the integration of TV-GFRFs with the fundamental frequencies in the input as in (12). Also, the magnitude of each frequency component in the output spectrum is time dependent, because of the parametric TV effects in the TV-NARX model.

Apart from providing an analytical relationship between input and output spectra, the TV-OFRF (12) also presents an important approach for the time–frequency analysis of complex nonstationary signals, especially when the time–frequency spectrum of the input signal is easily accessible. In this paper, it is assumed that the input can be treated as a "linear" signal [38], and hence, the time–frequency representation of the input $U(f,t)$ can be obtained by employing linear parametric approaches, such as TV-ARMA model [13].

V. Simulation and Application

In this section, a simulated discrete nonlinear time-varying system and a real EEG data set are given as examples to illustrate the proposed time-domain identification and frequency-domain analysis approaches. The first example demonstrates that the multiwavelet expansion method together with FROLS can accurately identify the true system structure and estimate the time-varying and time-invariant parameters. The identified TV model can then be mapped to the frequency domain using the proposed TV-GFRF and TV-OFRF concepts; the time–frequency characteristics of the system and output response can therefore be visualized and analyzed. The second example emphasizes that the proposed modeling and frequency-domain approaches can be successfully applied to real nonstationary data by using a relatively simple model. In addition, the output spectrum obtained from TV-OFRF implementation can provide more accurate time–frequency analysis results than the classical linear parametric or nonparametric approaches.

A. Artificial Data Modeling

The measurement data were generated from the following TV-NARX system:

$$y(k) = c_{1,0}(1,k)y(k-1) + c_{1,0}(2,k)y(k-2) + c_{0,1}(2,k)u(k-2) + c_{0,2}(1,2,k)u(k-1)u(k-2) + e(k) \tag{13}$$

where the time-varying and constant parameters are given as

$$c_{1,0}(1,k) = \begin{cases} 0.5, & 0 \le k\Delta t < 100\,\text{s} \\ 1, & 100 \le k\Delta t < 200\,\text{s} \\ 0.8, & 200 \le k\Delta t \le 600\,\text{s} \end{cases}, \quad \begin{matrix} c_{1,0}(2,k) = -0.3 \\ c_{0,1}(2,k) = 0.1 \end{matrix}$$

$$c_{0,2}(1,2,k) = \begin{cases} 0.4, & 0 \le k\Delta t < 300\,\text{s} \\ 0.4 + 0.2\sin(0.02\pi k\Delta t), & 300 \le k\Delta t < 600\,\text{s} \end{cases}$$

The input $u(k)$ was given as $u(k) = A\sin(\omega_1 k) + A\sin(\omega_2 k)$ with sampling time $\Delta t = 0.5$ s ($f_s = 2$ Hz), where $A = 2$, $\omega_1 = 0.2 \times 2\pi$, and $\omega_2 = 0.3 \times 2\pi$. $e(k)$ was the additive Gaussian independent identically distributed (i.i.d.) noise, with zero mean and variance 0.0025. For simplicity, the initial candidate model terms were set as $\{y(k-1),\ y(k-2),\ u(k-1),\ u(k-2),\ y(k-1)^2, y(k-1)y(k-2),\ y(k-2)^2, u(k-1)^2, u(k-1)u(k-2), u(k-2)^2\}$ with corresponding parameters $c_{1,0}(1,k)$, $c_{1,0}(2,k)$, $c_{0,1}(1,k)$, $c_{0,1}(2,k)$, $c_{2,0}(1,1,k)$, $c_{2,0}(1,2,k)$, $c_{2,0}(2,2,k)$, $c_{0,2}(1,1,k)$, $c_{0,2}(1,2,k)$, $c_{0,2}(2,2,k)$. Multiwavelet basis functions (i.e., a combination of third- to fifth-order B-spline bases [13]) were then used to expand all the time-varying parameters and transform them into constant kernel parameters. Then, the FROLS algorithm was applied to select the appropriate model structure from the expanded candidate terms and estimate the parameters. After selection and estimation, the original time-varying parameters can be reconstructed and are displayed in Fig 1.

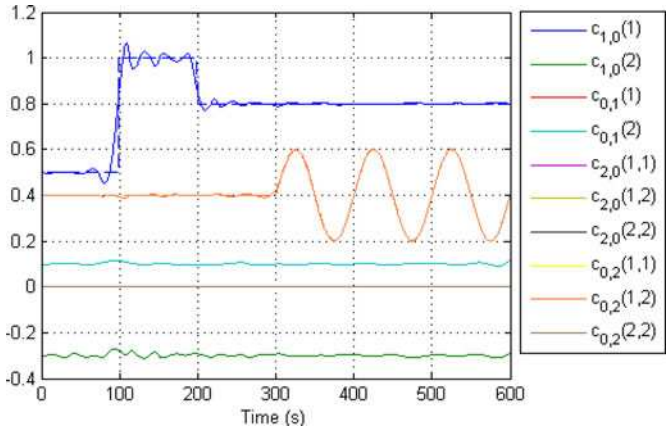

Fig. 1. Parameter estimates of candidate model terms using multiwavelets and the FROLS approach; the true TV parameter values are shown as dashed lines.

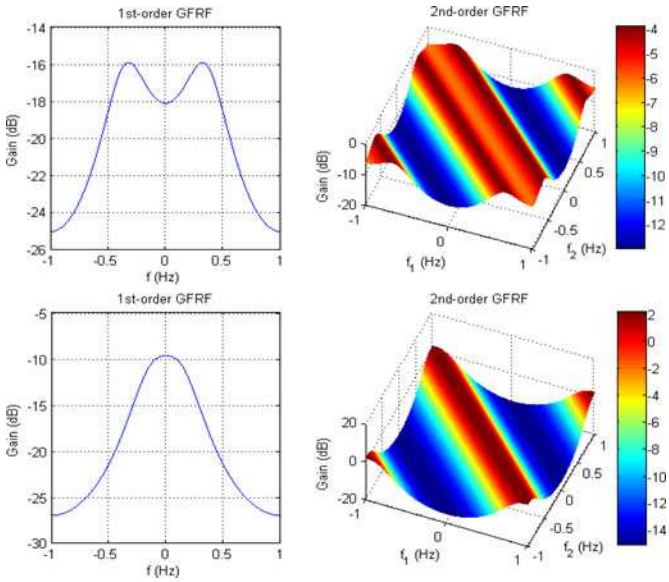

Fig. 2. Gains of first- and second-order GFRFs at (upper plots) 50 s and (lower plots) 150 s in time.

Fig. 1 demonstrates that the multiwavelet with FROLS approach can accurately estimate and track the time-varying parameters, estimate time-invariant parameters, and set all the other parameters of the "redundant" candidate terms to 0. This result indicates that the proposed approach can successfully identify the model structure for a discrete-time, time-varying nonlinear system, and accurately estimate the model parameters (with normalized mean squared error (NMSE) 8.58e–4). Based on the identified time-domain model, the first- and second-order TV-GFRFs can be obtained from (4). Since the system nonlinearity is purely introduced from the input (in second-order), higher order nonlinear effects, such as third-order TV-GFRF, will not be present in this example. To illustrate the effects of parametric time variations with respect to the system FRFs, the first- and second-order TV-GFRFs at two sampling time instances are shown in Fig. 2.

Fig. 2 shows that at 50 s there are two peaks in the first-order GFRF at $f = \pm 0.3$ Hz, and there are two ridges in the

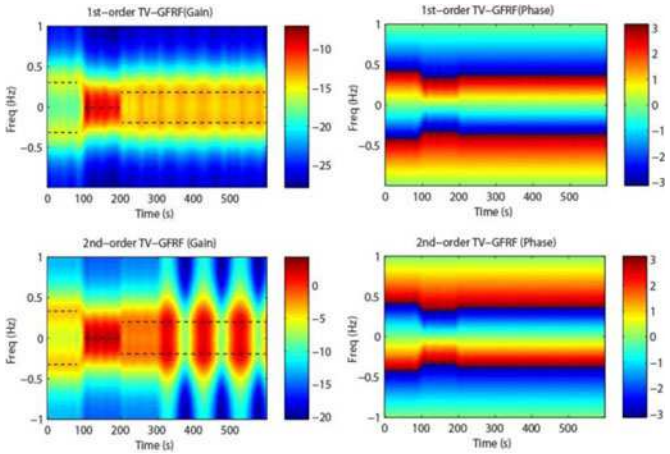

Fig. 3. Contours of the (upper) first-order TV-GFRF (H_1) and (lower) the averaged second-order TV-GFRF (H_2) (left) gain and (right) phase plots based on the estimated TV-NARX model. Ridges are marked with black dashed lines. The magnitudes in the gain plots are in decibels and the magnitudes in the phase plots are in radians.

second-order GFRF along $f_1 + f_2 = \pm 0.3$ Hz; at 150 s, only one peak is present at $f = 0$ Hz and one ridge along $f_1 + f_2 = 0$ Hz. This indicates that the parametric time-varying can affect the positions of peaks and ridges in the (TV-)GFRFs while the direction of the ridges is unaffected. To further investigate the influence of the time variations in both the linear and the nonlinear model terms to the TV-GFRFs, the first- and averaged second-order TV-GFRFs (along the $f_1 + f_2 = C_i$ direction) are computed from (10). The contours of corresponding gain and phase plots are illustrated in Fig. 3.

Fig. 3 presents the complete time–frequency characteristics of the identified time-varying system and clearly demonstrates how the features in TV-GFRFs depend on the time-varying parameters. The positions of ridges in both first- and second-order TV-GFRFs purely depend on the parameters of the linear output terms (i.e., $c_{1,0}(1,k)$ and $c_{1,0}(2,k)$) and their variations are only affected by $c_{1,0}(1,k)$, which is the only time-varying parameter in the linear terms. The gain magnitudes of first-order GFRF only depend on the linear input and output terms (again $c_{1,0}(1,k)$); however, the magnitudes of the ridges in the second-order TV-GFRF are affected by the time-varying parameters of both the linear and nonlinear terms (i.e., $c_{1,0}(1,k)$ and $c_{0,2}(1,2,k)$). The right-hand plots in Fig. 3 demonstrate that the phase of the first- and second-order TV-GFRFs can be quite different, but the time variations only depend on the time-varying parameters in the linear terms. The simulation results here confirm the theoretical analysis especially Proposition 1, and such visualization of TV-GFRFs provides important information in practice. For example, given the positions and magnitudes of the ridges in the TV-GFRFs, it is possible to predict when there are significant intermodulation effects on the output response if the sum of the frequency components in the input excitation is close to a specific ridge and how strong these effects are, without actually computing the output spectrum.

To confirm the observation and analysis from TV-GFRFs, the output time-dependent spectrum can be computed based on the

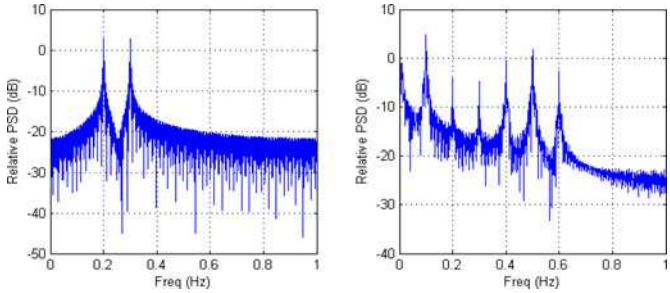

Fig. 4. (Left) Spectra of input and (right) output sequences using FFT.

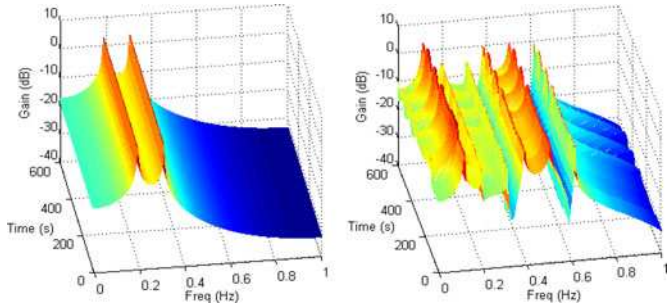

Fig. 5. Time–frequency spectral analysis of (left) input using TV-AR modeling and (right) output based on TV-NARX model and TV-OFRF theory.

proposed TV-OFRF theory. According to (12), the TV-OFRF of identified TV-NARX model can be expressed as

$$Y(f,t) = H_1(f,t) \cdot U(f,t) + 1/\sqrt{2} \times \int_{f_1+f_2=f} H_2(f_1,f_2,t) \cdot U(f_1,t) \cdot U(f_2,t) df \quad (14)$$

where the TV-GFRFs ($H_1(f,t)$ and $H_2(f_1,f_2,t)$) are available from the aforementioned analysis; the input-time-dependent spectrum $U(f_1,t)$ can be obtained from the parametric TV-AR modeling of the input signal $u(t)$. After the TV-AR model is identified in time, it can be mapped into the time–frequency domain [13]. For comparison, the time-invariant spectra of the input and output signals using a fast Fourier transform (FFT) are given in Fig. 4, and the time–frequency spectral analysis of input and output sequences using proposed approaches are given in Fig. 5.

Fig. 4 indicates that the classical FFT can well identify the two frequencies (0.2 and 0.3 Hz) in the input sequence. Due to the strong intermodulation effects, more frequency components are identified in the output spectrum, for example, $2f_1 = 0.4$ Hz, $f_1 + f_2 = 0.5$ Hz, $2f_2 = 0.6$ Hz, and $f_2 - f_1 = 0.1$ Hz. These intermodulation frequencies are with even higher magnitudes compared with the fundamental frequencies, indicating strong nonlinearity in the system. However, FFT-based spectrum analysis cannot reveal any time-dependent information, even if the output sequence is known to be nonstationary. Fig. 5 presents the time–frequency analysis results using the proposed parametric modeling approach. The time-dependent input spectrum based on TV-AR (i.e., fifth-order AR) model is given in the left plot. Two fundamental frequencies can be identified with constant magnitudes over time, which indicates that the input signal is

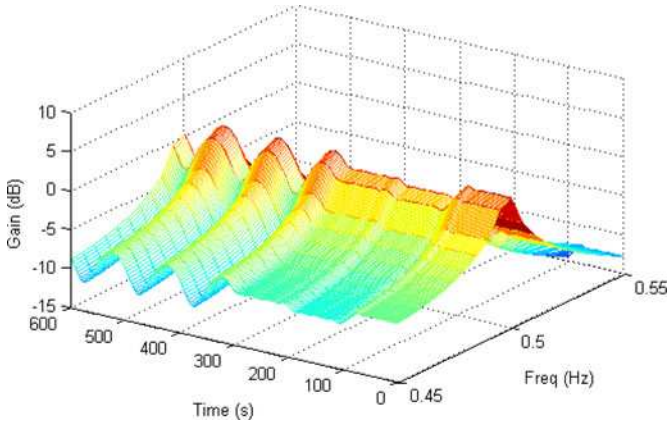

Fig. 6. Fragment of the output time–frequency spectrum given in Fig. 5 right plot.

time invariant. Based on the TV-OFRF expression (14), the output time–frequency spectrum is computed and given in the right plot. The same frequencies are identified as in the FFT-based result; but, more importantly, for each frequency component, the magnitude is time varying. A closer inspection with respect to a specific frequency, i.e., $f_1 + f_2 = 0.5$ Hz, is given in Fig. 6.

Notice that the spectrum at this frequency $f_1 + f_2 = 0.5$ Hz is time varying, and such variation essentially depends on the magnitude change in the second-order TV-GFRF (see Fig. 3) at this specific frequency (i.e., 0.5 Hz). Such dependency can be explained from the TV-OFRF expression (14), especially when the magnitudes of second-order TV-GFRF are even higher than the first-order TV-GFRF (as shown in Fig. 3). All the simulation results confirm the theoretical analyses; the parametric characteristics of the TV-NARX model determine the frequency response of the nonstationary system (TV-GFRFs), while the features in the TV-GFRFs together with input spectrum determine the characteristics of the output spectrum.

B. Intracranial EEG Example

EEG signals are known to exhibit strong nonstationary and nonlinear effects [39], [40]. However, most existing time and frequency-domain analysis methods for EEG signals are based on linear algorithms that can never reveal nonlinear frequency-domain features such as intermodulation, energy transfer, and other complex nonlinear effects. In this example, a fragment of an intracranial EEG recording will be used as an example to demonstrate the application of a TV-NARX model-based analysis. The EEG signals are recorded in two intracranial channels with a sampling rate of 250 Hz. One is measured in the left brain (i.e., left subtemporal contacts, LsubT2-LsubT3), and the other in the right brain (i.e., RsubT2-RsubT3). The former signal is treated as the input, while the latter is regarded as the output signal. The time series of input and output signals together with the spectra computed using a conventional FFT routine are illustrated in Figs. 7 and 8. For illustration and modeling simplicity, we only focus on the low-frequency range, i.e., 0–20 Hz, in this study.

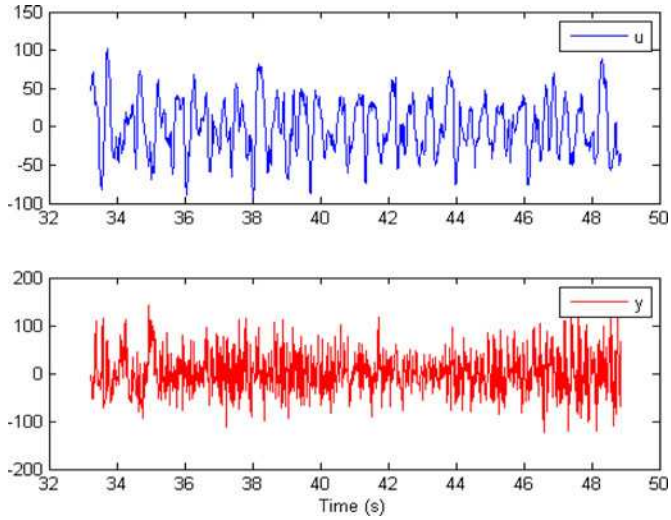

Fig. 7. Intracranial EEG recordings of (upper) input and (lower) output channels.

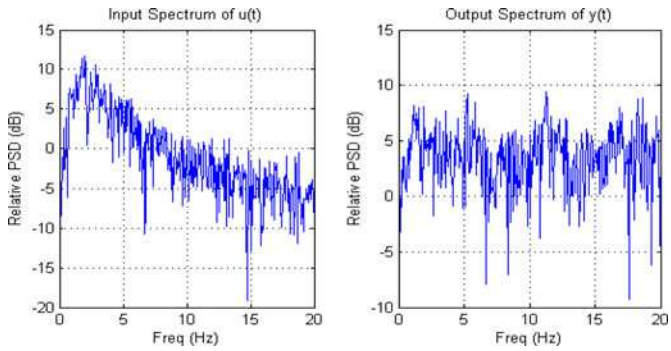

Fig. 8. Spectra of (left) input and (right) output EEG signals using FFT.

The time series of input and output signals in Fig. 7 show that the EEG in left brain has relatively slow periodic oscillations, while the EEG recorded from right brain contains higher frequencies. This is more clearly shown in the frequency domain in Fig. 8 where the input has a low-frequency component around 2 Hz, and the output spectrum has a broader spread of frequency components at 2, 5, 11, and 18 Hz. The different frequency components between input and output spectra suggest the existence of nonlinearity. However, classic FFT-based spectral analysis cannot reveal any time-dependent information. The model-based approach was then applied. A TV-NARX model with second-order nonlinearity and maximum lags of 6 in both input and output terms was used to fit to the EEG data. By using a multiwavelet expansion of TV parameters and FROLS selection, an appropriate model structure was selected and the TV parameters were estimated (with NMSE $= 0.141$). TV-GFRFs were then computed based on the identified TV-NARX model. The gain plots of first-order and averaged second-order TV-GFRFs are shown in Fig. 9.

Fig. 9 shows that the "ridges" in TV-GFRFs are mainly distributed in the frequency range of 10–20 Hz, and the gain magnitudes are relatively small in the low-frequency range of 0–5 Hz. As the energy of input signal is distributed around 2 Hz

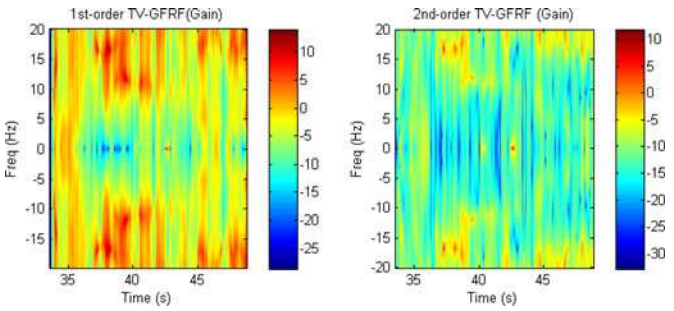

Fig. 9. Contours of the first-order TV-GFRF (H_1) (left) and the averaged second-order TV-GFRF (H_2) (right) gain plots based on the identified TV-NARX model for EEG signals.

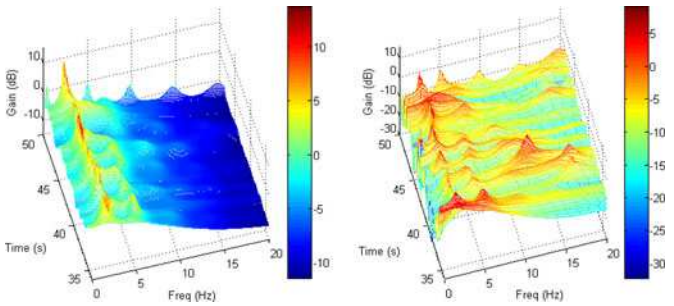

Fig. 10. Time–frequency spectra of (left) input and (right) output EEG recordings.

according to spectral analysis, the system appears to transfer the energy from low frequencies to higher frequencies, which is an important feature of nonlinear systems known as energy transfer [41]. The nonstationarity of the EEG recording is revealed as high gain magnitudes between 37 and 42 s in both first and second-order TV-GFRFs. This indicates strong intermodulation effects during this time interval where the higher frequency components at 11 and 18 Hz appear in the right brain. To confirm such observations, the time–frequency spectrum of input is first computed using TV-AR (with 18th order) model as in left plot of Fig. 10. Together with the TV-GFRFs, the time–frequency spectrum of the output signal can be obtained using TV-OFRF (12) and is given in the right plot of Fig. 10.

The time–frequency analysis of the input EEG shows that consistent "peaks" are observed around 2 Hz along all the time instants, which confirms the FFT-based analysis and indicates the left brain EEG is relatively stationary at this time interval. The time–frequency spectrum of output EEG identifies significantly more frequency components, for example, around 2 and 5 Hz, and several "peaks" are observed at 11 and 18 Hz around 40 s in time, which explains the high magnitudes in the TV-GFRF gain plots at this time period. The output time–frequency result confirms the observations in the system's analysis, identifies consistent frequency components with the FFT, and provides extra time-dependent information.

Additionally, the high-resolution time–frequency analysis results obtained here using a nonlinear model-based approach cannot be easily reproduced using standard linear parametric or nonparametric time–frequency approaches. For instance, a parametric TV-AR model-based approach can identify the time–

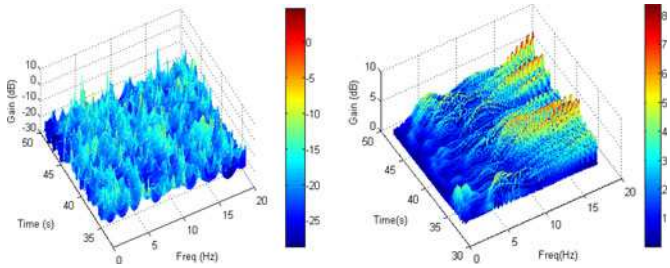

Fig. 11. Time–frequency spectral analysis of output sequence using (left) TV-AR-model-based approach and (right) wavelet transformation.

frequency spectrum of a "linear" TV signal, such as the input signals in both examples. Nevertheless, if a TV-AR model is directly applied to the output sequence that is nonlinear and nonstationary, it may provide a good fit in time but cannot reproduce the "true" frequency components in the time–frequency domain as shown in the left plot in Fig. 11. This is because an AR(MA) model can only be used to "explain" a "linear" signal [38]. Additionally, some widely used nonparametric time–frequency approaches, such as wavelet transformation, can also fail to identify the components that are close in frequency, due to the natural properties of wavelet basis functions, as shown in the right plot of Fig. 11. Other "local" or "sliding-window" approaches, such as short time Fourier transform (STFT) [42], may produce satisfactory results for some nonlinear and nonstationary signals; however, the selection of an appropriate window size is problem dependent and the computational complexity often limits their application.

VI. Conclusion

The frequency-domain analysis of a nonlinear and nonstationary system is an important but challenging task that has not yet been systematically investigated in the literature. In this study, a parametric-modeling-based framework is proposed by first modeling the unknown system using a TV-NARX model. The identified time-domain model can then be mapped into the frequency domain based on the TV-GFRF formulation; therefore, the nonlinear features can be tracked in frequency. Based on the characteristic analysis of the TV-GFRFs, the high-dimensional nonlinear frequency features can be visualized in a two-dimensional time–frequency space, which greatly facilitates the practical analysis of a nonstationary process in the frequency domain. In addition, the analytical expression describing the input and output time–frequency spectra is introduced based on the TV-OFRF concept. As a result, the time–frequency spectrum of a complex nonlinear nonstationary signal can be computed from the spectrum of a relatively simple input signal.

The proposed approach can potentially be applied for the spectral and nonlinear frequency analysis of a wide range of nonstationary signals, such as physiological and biochemical signals. The EEG data used in this paper are seizure-free and only used to demonstrate the accuracy of the algorithm in identifying the nonlinear frequency components in real nonstationary data. Nevertheless, the proposed time–frequency analysis method has great potential to be applied to identify, diagnose,

or even predict the pathological conditions, such as epilepsy seizures, in the electrophysiological signals.

REFERENCES

[1] D. A. George, "Continuous nonlinear systems," MIT Res. Lab. Electron., Cambridge, MA, USA, Tech. Rep. 335, 1959.

[2] S. Boyd, Y. S. Tang, and L. O. Chua, "Measuring Volterra kernels," *IEEE Trans. Circuits Syst.*, vol. CAS-30, no. 8, pp. 571–577, Aug. 1983.

[3] L. O. Chua and Y. Liao, "Measuring Volterra kernels (II)," *Int. J. Circuit Theory Appl.*, vol. 17, pp. 151–190, 1989.

[4] S. A. Billings and K. M. Tsang, "Spectral analysis for non-linear systems, Part I: Parametric nonlinear spectral analysis," *J. Mech. Syst. Signal Process.*, vol. 3, no. 4, pp. 319–339, 1989.

[5] J. C. Peyton Jones and S. A. Billings, "A recursive algorithm for computing the frequency response of a class of nonlinear difference equation models," *Int. J. Control*, vol. 50, no. 5, pp. 1925–1940, 1989.

[6] S. A. Billings and J. C. Peyton Jones, "Mapping nonlinear integro-differential equations into the frequency domain," *Int. J. Control*, vol. 52, pp. 863–879, 1990.

[7] Z. Q. Lang and S. A. Billings, "Output frequencies of nonlinear systems," *Int. J. Control*, vol. 67, pp. 713–730, 1997.

[8] Z. Q. Lang, S. A. Billings, R. Yue, and J. Li, "Output frequency response function of nonlinear Volterra systems," *Automatica*, vol. 43, pp. 805–816, 2007.

[9] W. Fitzgerald, R. Smith, A. Walden, and P. Young, *Nonlinear and Nonstationary Signal Processing*. Cambridge, U.K.: Cambridge Univ. Press, 2000.

[10] L. Ljung and T. Soderstrom, *Theory and Practice of Recursive Identification*. Cambridge, MA: MIT Press, 1983.

[11] L. Ljung and S. Gunnarsson, "Adaptation and tracking in system identification—A survey," *Automatica*, vol. 26, no. 1, pp. 7–21, 1990.

[12] R. Zou and K. H. Chon, "Robust algorithm for estimation of time-varying transfer functions," *IEEE Trans. Biomed. Eng.*, vol. 51, no. 2, pp. 219–228, Feb. 2004.

[13] H. L. Wei, S. A. Billings, and J. Liu, "Time-varying parametric modeling and time-dependent spectral characterization with applications to EEG signals using multiwavelets," *Int. J. Modeling Identification Control*, vol. 9, no. 3, pp. 215–224, 2010.

[14] Z. G. Zhang, Y. S. Hung, and S. C. Chan, "Local polynomial modeling of time-varying autoregressive models with application to time–frequency analysis of event-related EEG," *IEEE Trans. Biomed. Eng.*, vol. 58, no. 3, pp. 557–566, Mar. 2011.

[15] C. M. Ting, S. H. Salleh, Z. M. Zainuddin, and A. Bahar, "Spectral estimation of nonstationary EEG using particle filtering with application to event-related desynchronization (ERD)," *IEEE Trans. Biomed. Eng.*, vol. 58, no. 2, pp. 321–331, 2011.

[16] Y. Li, H. L. Wei, S. A. Billings, and P. G. Sarrigiannis, "Time-varying model identification for time–frequency feature extraction from EEG data," *J. Neurosci Methods*, vol. 196, no. 1, pp. 151–158, 2011.

[17] H. Peng, K. Nakano, and H. Shioya, "Nonlinear predictive control using neural nets-based local linearization ARX model-stability and industrial application," *IEEE Trans. Control. Syst. Technol.*, vol. 15, no. 1, pp. 130–143, Jan. 2007.

[18] F. N. Chowdhury, "Input–output modeling of nonlinear systems with time-varying linear models," *IEEE Trans. Autom. Control*, vol. 45, no. 7, pp. 1355–1358, Jul. 2000.

[19] M. Iatrou, T. W. Berger, and V. Z. Marmarelis, "Modeling of nonlinear nonstationary dynamic systems with a novel class of artificial neural networks," *IEEE Trans. Neural Netw.*, vol. 10, no. 2, pp. 327–339, Mar. 1999.

[20] Y. Zhong, K. M. Jan, K. H. Ju, and K. H. Chon, "Representation of time-varying nonlinear systems with time-varying principal dynamic modes," *IEEE Trans. Biomed. Eng.*, vol. 54, no. 11, pp. 1983–1992, Nov. 2007.

[21] I. J. Leontaritis and S. A. Billings, "Input–output parametric models for nonlinear systems, Part I: Deterministic nonlinear systems," *Int. J. Control*, vol. 41, pp. 303–328, 1985.

[22] S. Chen and S. A. Billings, "Representations of non-linear systems: The NARMAX model," *Int. J. Control*, vol. 49, no. 3, pp. 1012–32, 1989.

[23] S. Chen, S. A. Billings, and W. Luo, "Orthogonal least squares methods and their application to nonlinear system identification," *Int. J. Control*, vol. 50, no. 5, pp. 1873–1896, 1989.

[24] S. A. Billings, S. Chen, and M. J. Korenberg, "Identification of MIMO nonlinear systems using a forward-regression orthogonal estimator," *Int. J. Control*, vol. 49, no. 6, pp. 2157–2189, 1989.

[25] R. Zou, H. Wang, and K. H. Chon, "A robust time-varying identification algorithm using basis functions," *Ann. Biomed. Eng.*, vol. 31, pp. 840–853, Jul./Aug. 2003.

[26] M. K. Tsatsanis and G. B. Giannakis, "Time-varying system identification and model validation using wavelets," *IEEE Trans. Signal Process.*, vol. 41, no. 12, pp. 3512–3523, Dec. 1993.

[27] M. Niedzwiecki and T. Klaput, "Fast recursive basis function estimators for identification of time-varying processes," *IEEE Trans. Signal Process.*, vol. 50, no. 8, pp. 1925–1934, Aug. 2002.

[28] Y. Li, H. L. Wei, and S. A. Billings, "Identification of time-varying systems using multi-wavelet basis functions," *IEEE Trans. Control. Syst. Technol.*, vol. 19, no. 3, pp. 656–663, May 2011.

[29] N. J. Mars and F. H. Lopes da Silva, "Propagation of seizure activity in kindled dogs," *Electroencephalogr. Clin. Neurophysiol.*, vol. 56, pp. 194–209, 1983.

[30] R. Q. Quiroga, A. Kraskov, T. Kreuz, and P. Grassberger, "Performance of different synchronization measures in real data: A case study on electroencephalographic signals," *Phys. Rev. E*, vol. 65, p. 041903, 2002.

[31] M. Schetzen, *The Volterra and Wiener Theories of Nonlinear Systems*. Chichester, U.K.: Wiley, 1980.

[32] J. C. Peyton Jones and S. A. Billings, "A recursive algorithm for computing the frequency response of a class of nonlinear difference equation models," *Int. J. Control*, vol. 50, no. 5, pp. 1925–1940, 1989.

[33] S. A. Billings and K. M. Tsang, "Spectral analysis for non-linear systems, Part II: Interpretation of non-linear frequency response functions," *J. Mech. Syst. Signal Process.*, vol. 3, no. 4, pp. 341–359, 1989.

[34] S. A. Billings and K. M. Tsang, "Spectral analysis for non-linear systems, Part III: Case study examples," *J. Mech. Syst. Signal Process.*, vol. 4, no. 1, pp. 3–21, 1990.

[35] R. Yue, S. A. Billings, and Z. Q. Lang, "An investigation into the characteristics of non-linear frequency response functions. Part 1: Understanding the higher dimensional frequency spaces," *Int. J. Control*, vol. 78, no. 13, pp. 1031–1044, Sep. 2005.

[36] R. Yue, S. A. Billings, and Z. Q. Lang, "An investigation into the characteristics of non-linear frequency response functions. Part 2: New analysis methods based on symbolic expansions and graphical techniques," *Int. J. Control*, vol. 78, no. 14, pp. 1130–1149, Sep. 2005.

[37] X. J. Jing, Z. Q. Lang, S. A. Billings, and G. R. Tomlinson, "The parametric characteristic of frequency response functions for nonlinear systems," *Int. J. Control*, vol. 79, no. 12, pp. 1552–1564, Dec. 2006.

[38] J. Theiler, S. Eubank, A. Longtin, B. Galrikian, and J. Farmer, "Testing for nonlinearity in time series: The method of surrogate data," *Physica D*, vol. 58, pp. 77–94, 1992.

[39] N. V. Thakor and S. Tong, "Advances in quantitative electroencephalogram analysis methods," *Annu. Rev. Biomed. Eng.*, vol. 6, pp. 453–495, 2004.

[40] A. Y. Kaplan, A. A. Fingelkurts, A. A. Fingelkurts, S. V. Borisov, and B. S. Darkhovsky, "Nonstationary nature of the brain activity as revealed by EEG/MEG: Methodological, practical and conceptual challenges," *Signal Process*, vol. 85, no. 11, pp. 2190–2212, 2005.

[41] Z. Q. Lang and S. A. Billings, "Energy transfer properties of nonlinear systems in the frequency domain," *Int. J. Control*, vol. 78, no. 5, pp. 345–362, 2005.

[42] M. R. Portnoff, "Time–frequency representation of digital signals and systems based on short-time fourier analysis," *IEEE Trans. Acoust., Speech, Signal Process*, vol. ASSP-28, no. 1, pp. 55–69, Feb. 1980.

Authors' photographs and biographies not available at the time of publication.